PHYSICAL REVIEW C VOLUME 24, NUMBER 4 OCTOBER 1981

Delta-hole formalism of pion-nucleus single charge exchange scattering

M. Hirata

Department of Physics, Hiroshima University, Hiroshima, Japan and Schweizerisches Institut für Nuklearforschung, Villigen, Switzerland

(Received 2 December 1980)

The pion-nucleus single charge exchange scattering matrix is described by the nonstatic theory based on the delta-hole formalism which is quite successful for the pion-nucleus elastic scattering in the (3,3) resonance energy region. The calculated excitation function of the $^{13}C(\pi^+, \pi^0)^{13}N_{g.s.}$ charge exchange scattering cross section becomes flat between the pion kinetic energies 70 and 230 MeV, but the theoretical integrated cross sections are roughly a factor of 3 less than the observed ones. The observed shape of angular distribution at 150 MeV is well reproduced by our theory, although the absolute values of the calculated angular distribution are slightly smaller than the measurements.

[NUCLEAR REACTIONS Pion-nucleus single charge exchange scattering. Delta-hole formalism, pion energy 70–230 MeV.]

I. INTRODUCTION

The $^{13}C(\pi^+, \pi^0)^{13}N_{g.s.}$ charge exchange (CE) scattering theoretically looks like a simple reaction to reproduce experimental data. Considering this process in the distorted-wave impulse approximation (DWIA), only the monopole type transition density contributes to this CE scattering. Most theories, however, predict a dip in the excitation function of the $^{13}C(\pi^+, \pi^0)^{13}N_{g.s.}$ integrated cross section in the (3,3) resonance region, whereas experiment[1] shows the integrated cross section to be roughly independent of energy, and also shows that the observed cross sections are roughly a factor of 2 to 5 larger than the theoretical predictions. Various theoretical methods[2-9] were proposed to attack the above problem. See Ref. 10 for a review of the theoretical methods. The pion-nucleus higher order optical potential, especially the contribution from the true pion absorption to the optical potential and the Pauli-quenching effect for the delta, have not been seriously considered in every theory. The true pion absorption cross section accounts for about 50 percent of the total inelastic cross section. Therefore, the contribution from this channel to the optical potential cannot be neglected. The energy dependence of the true pion absorption cross section is different from that of the quasi-elastic cross section. Therefore, the inclusion of the higher order optical potential will change the shape of the excitation function of the $^{13}C(\pi^+, \pi^0)^{13}N_{g.s.}$ CE scattering cross section.

In this paper the nonstatic theory based on the delta-hole formalism[11,12] is applied to charge exchange scattering. This theory is quite successful in describing the pion-nucleus elastic scattering in the (3,3) resonance energy region. The isobar doorway model[13] had already been applied to the charge exchange scattering.[14] Although it reproduced the data quite well, the calculation of Ref. 14 was phenomenological, and the assumptions introduced to obtain the final equation were not always physically understandable. It is necessary that the problem of the $^{13}C(\pi^+, \pi^0)^{13}N_{g.s.}$ CE scattering be reexamined using a more rigorous formula than that of Ref. 14.

Our calculation includes recoil and binding corrections to the pion-nucleon amplitude which are used to define the Hamiltonian of the delta. Furthermore, the spreading potential for the delta, and the Pauli-quenching effect for the decay of the delta into a pion and a nucleon, are taken into account. The spreading potential represents the coupling effect of the delta-hole states to the more complicated states.

In Sec. II the CE scattering matrix for the $^{13}C(\pi^+, \pi^0)^{13}N_{g.s.}$ is described by the delta-hole formalism. The results of our analysis and the next step to obtain the absolute cross section of the $^{13}C(\pi^+, \pi^0)^{13}N_{g.s.}$ CE scattering are discussed in Sec. III. We conclude with a short summary in Sec. IV.

II. OUTLINE OF FORMALISM

The nonstatic theory[11,12] is applied to the charge exchange scattering (CE). Miller and Spencer[7] have shown that the effect of Coulomb distortion on the charge-exchange reactions is very small for pion energies greater than or equal to 100 MeV. Therefore, the isospin formalism is used here by omitting the Coulomb interaction between a pion and a nucleus and the mass differences of various charged particles. Then the CE scattering matrix T_{10} in the case of the $^{13}C(\pi^+, \pi^0)^{13}N_{g.s.}$ scattering is given by

$$T_{10}(\vec{k}',\vec{k};E)=\frac{\sqrt{2}}{3}[T_{3/2}(\vec{k}',\vec{k};E)-T_{1/2}(\vec{k}',\vec{k};E)], \tag{1}$$

where $\vec{k}$ and $\vec{k}'$ are the initial and the final pion momenta, respectively, and $T_{3/2}$ and $T_{1/2}$ are the scattering matrices of the isospins $t=\frac{3}{2}$ and $t=\frac{1}{2}$, respectively. Thus the calculation of the CE scattering becomes the same as that of the elastic scattering in the isospin space. In this case, the treatment of Ref. 12 can be easily extended to the pion and odd nucleus system. Our formalism is briefly explained.

The scattering matrix T_t for the isospin t is written in terms of the optical potential U_t for the isospin t as

$$T_t=U_t+U_t\frac{P}{e}T_t, \tag{2}$$

where P is the projection operator which projects out the lowest state of the nucleus which is coupled to the pion to make the total isospin t. The propagator e is given by

$$e=(E-H_A)^2-p^2-\mu^2, \tag{3}$$

where H_A is the Hamiltonian for the target nucleus consisting of A nucleons, and p and μ are the momentum and the mass of the pion. The potential U_t is divided into two parts,

$$U_t=U_{tbg}+U_{t33}. \tag{4}$$

The first part is built from partial waves other than the P_{33} wave in the pion-nucleon scattering, and is represented by U_{tbg}. It is replaced by the usual first order optical potential $U_{tbg}^{(1)}$. The second part consists of the P_{33} partial wave, and is represented by U_{t33}.

In the following, we give an outline of the construction of U_{t33}. Our starting point is the optical potential expansion of the Watson multiple scattering theory. The optical potential is written as

$$U=\sum_{i=1}^{A}\tau_i+\sum_{i=j}^{A}\tau_i\frac{Q}{e}\tau_j+\cdots, \tag{5}$$

where $Q=1-P$. τ_i is defined by

$$\tau_i=V_i+V_i\frac{Q}{e}\tau_i, \tag{6}$$

where V_i is the interaction potential between a pion and the ith nucleon. First, U is approximated by $U^{(1)}=\sum_i\tau_i$. Let us now introduce the π-N scattering matrix for a nucleon in the target nucleus

$$t_i=V_i+V_i\frac{1}{e}t_i, \tag{7}$$

and the scattering matrix with the modified propagator e_Δ

$$t_{i\Delta}=V_i+V_i\frac{1}{e_\Delta}t_{i\Delta}, \tag{8}$$

where $e_\Delta=(E-H_\Delta)^2-[1+(E/M)]P_r^2-\mu^2$, and $H_\Delta=T_\Delta+V_\Delta+H_{A-1}$. Here, T_Δ is the kinetic operator of the π-N center of mass, and V_Δ the binding potential which is chosen so as to make the difference between t_i and $t_{i\Delta}$ as small as possible. So t_i is replaced by $t_{i\Delta}$. The suffix i is dropped from now on. The t matrix t_Δ in the momentum representation can be expressed as follows:

$$\langle\vec{k}',\vec{K}_N'|t_\Delta|\vec{k},\vec{K}_N\rangle$$
$$=g^*(\vec{\kappa}')\langle\vec{k}'+\vec{K}_N'|D^{-1}(E-H_\Delta)|\vec{k}+\vec{K}_N\rangle g(\vec{\kappa}), \tag{9}$$

where $\vec{\kappa}=(M\vec{k}-E\vec{K}_N)/(M+E)$ and $g(\vec{\kappa})=g\vec{T}^+\vec{S}^+\cdot\vec{\kappa}/(\kappa^2+a^2)$. The denominator function $D(E-H_\Delta)$ is expanded up to the first order in H_Δ,

$$D(E-H_\Delta)\approx D(E)-\gamma(E)H_\Delta, \tag{10}$$

where $D(E)=E-E_R(E)+(i/2)\Gamma_R(E)$ and $\gamma(E)=1-(\partial E_R/\partial E)+(i/2)(\partial\Gamma_R/\partial E)$. From Eqs. (6) and (7) τ is rewritten as

$$\tau=t-t\frac{P}{e}\tau\approx t_\Delta-t_\Delta\frac{P}{e}\tau. \tag{11}$$

The projection operator P is extended to include $P\to P+\sum_{PVt}|PVt\rangle\langle PVt|$ in order to take into account the Pauli-quenching effect for the decay of the isobar into a pion and a nucleon. $|PVt\rangle$ represents the Pauli-violating state. The direct product of the incident pion and the lowest state of the nucleus is expressed as $|\vec{k}Pt\rangle$, where P represents the lowest state of the nucleus. For the final state $\vec{k}$ is replaced by $\vec{k}'$. Using Eqs. (9) and (11), the optical potential U_{t33} is written, within the limit of the first and second order in the Pauli quenching effect, as

$$U_{t33}(\vec{k}',\vec{k};E)=\left\langle\vec{k}'Pt\left|\sum_i\tau_i\right|\vec{k}Pt\right\rangle$$
$$=\sum_{\substack{\Delta N\\ \Delta'N'}}F^*_{P\Delta'N'^{-1}t}(\vec{k}')\langle P\Delta'N'^{-1}t|[D(E-H_\Delta)-V_F-V_{\Delta-P}]^{-1}|P\Delta N^{-1}t\rangle F_{P\Delta N^{-1}t}(\vec{k})$$
$$+\delta_{t,3/2}\sum_{\Delta\Delta'}F^*_{\Delta'P}(\vec{k}')\langle\Delta'|[D(E-H_\Delta)-V_F]^{-1}|\Delta\rangle F_{\Delta P}(\vec{k}), \tag{12}$$

where $F_{P\Delta N^{-1}t}(\vec{k}) = \langle \Delta P N^{-1} t \,|\, g(\vec{\kappa}) \,|\, \vec{k} P t \rangle$ and $F_{\Delta P} = \langle \Delta \,|\, g(\vec{\kappa}) \,|\, \vec{k} P t = \frac{3}{2} \rangle$. The matrix elements of V_F and $V_{\Delta\text{-}P}$ are diagramatically shown in Figs. 1(a) and (b), respectively. The quantities V_F and $V_{\Delta\text{-}P}$ represent the Pauli-violation terms. The interaction $V_{\Delta\text{-}P}$ appears only in the pion-nonclosed shell nucleus scattering, and the matrix element of $V_{\Delta\text{-}P}$ depends on the isospin t and the total angular momentum J, where $\vec{J} = \vec{l}_\pi + \vec{j}_p$. It is known that the optical potential of Eq. (12) produces a much too pronounced resonance structure in the elastic cross section, the total cross section, and the real part of the forward amplitude.[12] The $P\Delta N^{-1}t$ states or the Δ states must be coupled to more complicated states. In order to take into account the coupling of the $P\Delta N^{-1}t$ states or the Δ states to those other states, we introduce the spreading potential W_s^t into the denominators in Eq. (12) phenomenologically, although recently a microscopic treatment for the spreading potential has been proposed.[15] For simplicity W_s^t is assumed to have the same shape and range as the potential V_Δ.

Now, the intermediate isobar-nuclear states $|P\Delta N^{-1}t\rangle$ and $|\Delta t = \frac{3}{2}\rangle$ are represented by $|dt\rangle$. Using Eqs. (1), (2), and (4) the CE scattering matrix T_{10}, like the $^{13}C(\pi^+, \pi^0)^{13}N_{g.s.}$, is written as

$$
\begin{aligned}
T_{10}(\vec{k}', \vec{k}; E) = {} & \frac{\sqrt{2}}{3}\left[T_{3/2}^{bg}(\vec{k}', \vec{k}; E) - T_{1/2}^{bg}(\vec{k}', \vec{k}; E)\right] \\
& + \frac{\sqrt{2}}{3}\Bigg\{ \sum_{\substack{d\,3/2 \\ d'\,3/2}} F^*_{d\,3/2}(\vec{k}') \langle d' \tfrac{3}{2} \Big| \Big[E - E_R(E) + \frac{i}{2}\Gamma_R(E) - \gamma(E) H_\Delta \\
& \qquad - V_F - V_{\Delta\text{-}P} - W_s^{3/2} - V_{\Delta\text{-}h} - V_{\Delta\text{-}\Delta h} \Big]^{-1} \Big| d\tfrac{3}{2} \rangle F_{d\,3/2}(\vec{k}) \\
& - \sum_{\substack{d\,1/2 \\ d'\,1/2}} F^*_{d\,1/2}(\vec{k}') \langle d' \tfrac{1}{2} \Big| \Big[E - E_R(E) + \frac{i}{2}\Gamma_R(E) - \gamma(E) H_\Delta - V_F - V_{\Delta\text{-}P} - W_s^{1/2} - V_{\Delta\text{-}h} \Big]^{-1} \Big| d\tfrac{1}{2} \rangle F_{d\,1/2}(\vec{k}) \Bigg\},
\end{aligned}
\tag{13}
$$

where

$$
F_{dt}(\vec{k}) = \int \frac{d\vec{q}}{(2\pi)^3} \langle dt \,|\, g(\vec{k}) \,|\, \psi_{\vec{\pi}\vec{k}}^{bg(+)}(\vec{q}) P t \rangle
$$

and $\psi_{\vec{\pi}\vec{k}}^{bg(+)}$ is the distorted wave due to $U_{tbg}^{(1)}$ of a pion. The matrix elements of $V_{\Delta\text{-}h}$ and $V_{\Delta\text{-}\Delta h}$ are shown by the diagrams of Figs. 2(a) and (b). The pion propagator includes $U_{tbg}^{(1)}$. The interactions $V_{\Delta\text{-}h}$ and $V_{\Delta\text{-}\Delta h}$ come from the pion multiple scattering by the nucleus. The pion receives the distortion by the residual nucleus through the interaction $V_{\Delta\text{-}\Delta h}$ during interaction with a nucleon outside the closed shell.

In Refs. 16 and 17 the difference in energy of the isospin $\frac{1}{2}$ and $\frac{3}{2}$ first-order optical potential was treated as a free parameter to fit the data. Once the static approximation is used, the physical origin of the difference does not become clear. The introduction into the theory of an ambiguous parameter which cannot sufficiently reproduce the energy dependence of the total cross section, the integrated cross section, and the true pion absorption cross section may lead to confusion. If we must look for the origin of such a difference in our formalism, the spreading potential W_s^t and the interaction $V_{\Delta\text{-}P}$ correspond to it.

III. CALCULATION RESULTS OF THE $^{13}C(\pi^+,\pi^0)^{13}N_{g.s.}$ CHARGE EXCHANGE SCATTERING

The scattering matrix T_{10} is decomposed into the partial wave amplitudes as usual. The ground

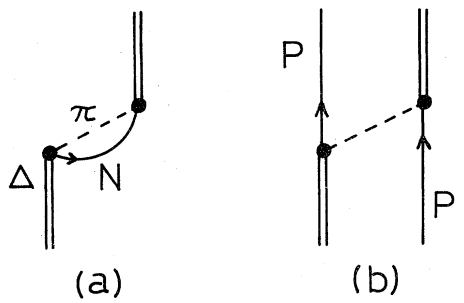

FIG. 1. (a) Fock diagram for Δ. (b) Diagram of the Δ-particle exchange interaction.

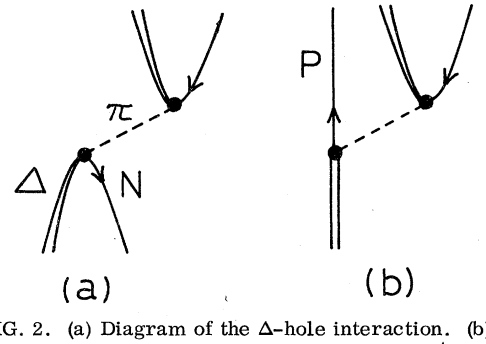

FIG. 2. (a) Diagram of the Δ-hole interaction. (b) Diagram of the interaction between Δ and $p\Delta N^{-1}$ configurations.

states of ^{13}C and ^{13}N are approximately described as the $P_{1/2}$ single particle state. The pion partial waves cannot couple each other because the total angular momenta of the initial and final target states are $\frac{1}{2}$. So, calculations become fairly simple. The energy-dependent resonance energy $E_R(E)$, the width $\Gamma_R(E)$, and the form factor range a are determined from the pion-nucleon P_{33} phase shifts. For V_Δ the same potential as the one for the nucleon which reproduces the binding energies of the single-particle orbits well is used. The binding potential V_Δ for delta is given by

$$V_\Delta(r) = -V_0[1+\tfrac{4}{3}\nu r^2]\exp(-\nu r^2)\,, \tag{14}$$

where $V_0 = 66$ MeV and $\nu = 0.34$ fm^{-2}. The spreading potential W_s^t is assumed to have the same shape and range as V_Δ,

$$W_s^t = (u_t + iv_t)[1+\tfrac{4}{3}\nu r^2]\exp(-\nu r^2)\,. \tag{15}$$

Although u_t and v_t should be determined from the forward amplitudes of the $\pi^+ - {}^{13}$C and $\pi^0 - {}^{13}$C elastic scatterings, the values determined from the $\pi^- - {}^{12}$C elastic scattering data[18] are used because of a lack of $\pi - {}^{13}$C elastic scattering data. It was assumed that $W_s^{3/2} = W_s^{1/2}$ because W_s^t itself is not well known, although $W_s^{3/2}$ is different from $W_s^{1/2}$ in general. A case where $W_s^{3/2}$ is not equal to $W_s^{1/2}$ is discussed in the latter half of this section.

The calculations are performed in a shell-model base. The hole and particle states are described by harmonic oscillator wave functions, and the isobar wave functions are expanded on the same base. Each denominator of the right-hand side in Eq. (13) is diagonalized in the one particle–one Δ–one hole and one Δ configuration spaces. The total cross sections, real parts of the forward amplitudes, and integrated elastic cross sections in the ^{12}C$(\pi^-, \pi^-)^{12}$C elastic scattering are calculated to fix the strength parameters of the spreading potential. The results are shown in Fig. 3. The complex values of the spreading potential W_s are given in Table I. The spreading potential shows the strong energy dependence. Very recently it has been pointed out that the introduction of a Δ-nucleus spin-orbit potential leads to a smooth energy dependence of the central part of the spreading potential.[19] We maintain our spreading potential form because the introduction of the Δ-nucleus spin-orbit potential does not influence the integrated CE scattering cross sections very much.[20] Now there is no free parameter to calculate the CE scattering cross sections. The integrated cross sections of the ^{13}C$(\pi^+, \pi^0)^{13}$N$_{g.s.}$ CE scattering are shown as the function of pion kinetic energy in Fig. 4. The dotted line shows the results obtained without the spreading potential. The excitation function has a small bump around the pion kinetic energy 100 MeV. In this case the elastic and total cross sections also have a too pronounced resonance structure. Next, the spreading potential is included, but since the complex strength of the spreading potential was fixed from the $\pi - {}^{12}$C elastic scattering without the

TABLE I. The complex strength of spreading potential fixed from the ^{12}C$(\pi^-, \pi^-)^{12}$C elastic scattering and used for the analysis of the ^{13}C$(\pi^+, \pi^0)^{13}$N$_{g.s.}$ charge exchange scattering.

T_π (MeV)	W_s (MeV)
70	$-3 - i44$
100	$-15 - i53$
150	$-27 - i47$
180	$-26 - i56$
230	$+14 - i50$

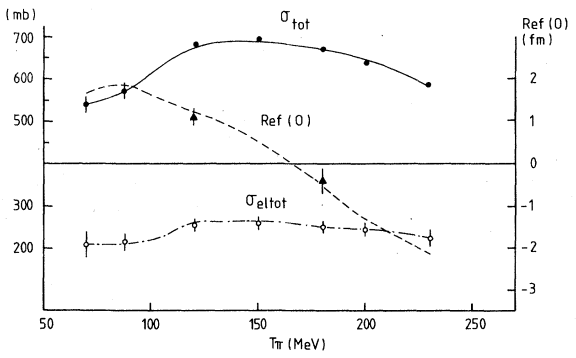

FIG. 3. Total cross sections, real parts of forward amplitudes, and integrated elastic cross sections in the $\pi^- - {}^{12}$C elastic scattering. The data are from Ref. 18. The theoretical curves are obtained by choosing u_s and v_s so as to fit σ_{tot} and Re$f(0)$.

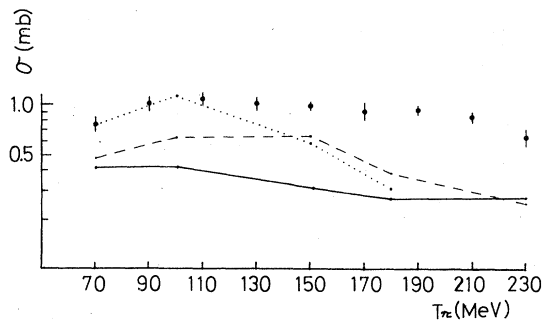

FIG. 4. The experimental and theoretical ^{13}C$(\pi^+, \pi^0)^{13}$N$_{g.s.}$ integrated cross sections as a function of the pion energy. The data are from Ref. 1. The dotted line is obtained without the spreading potential, and the dashed line with the spreading potential but without H_Δ and W_s^t for single Δ states. The solid line is obtained by including everything.

connection with a nucleon outside the closed shell, H_Δ and W_s^t are omitted for single Δ states (a kind of impulse approximation). In this case (the dashed line) the bump disappears. The variation of the integrated cross section is fairly strong between 150 and 180 MeV. This may be due to the fact that the free half width of the delta at 180 MeV is about 10 MeV larger than that at 150 MeV and the reduction of width from the Pauli-quenching is smaller at 180 than at 150 MeV. The full calculations are shown by the solid line. The variation of cross sections between the pion kinetic energies of 70 and 230 MeV is very small. The fully calculated cross sections become smaller than ones shown by the dashed line, and much smaller than the experimental ones. The inclusion of the spreading potential for the single delta states generally makes the amplitude of the isospin $\frac{3}{2}$ decrease. Up to now any reasonable theoretical calculation has not been able to reproduce the ex-

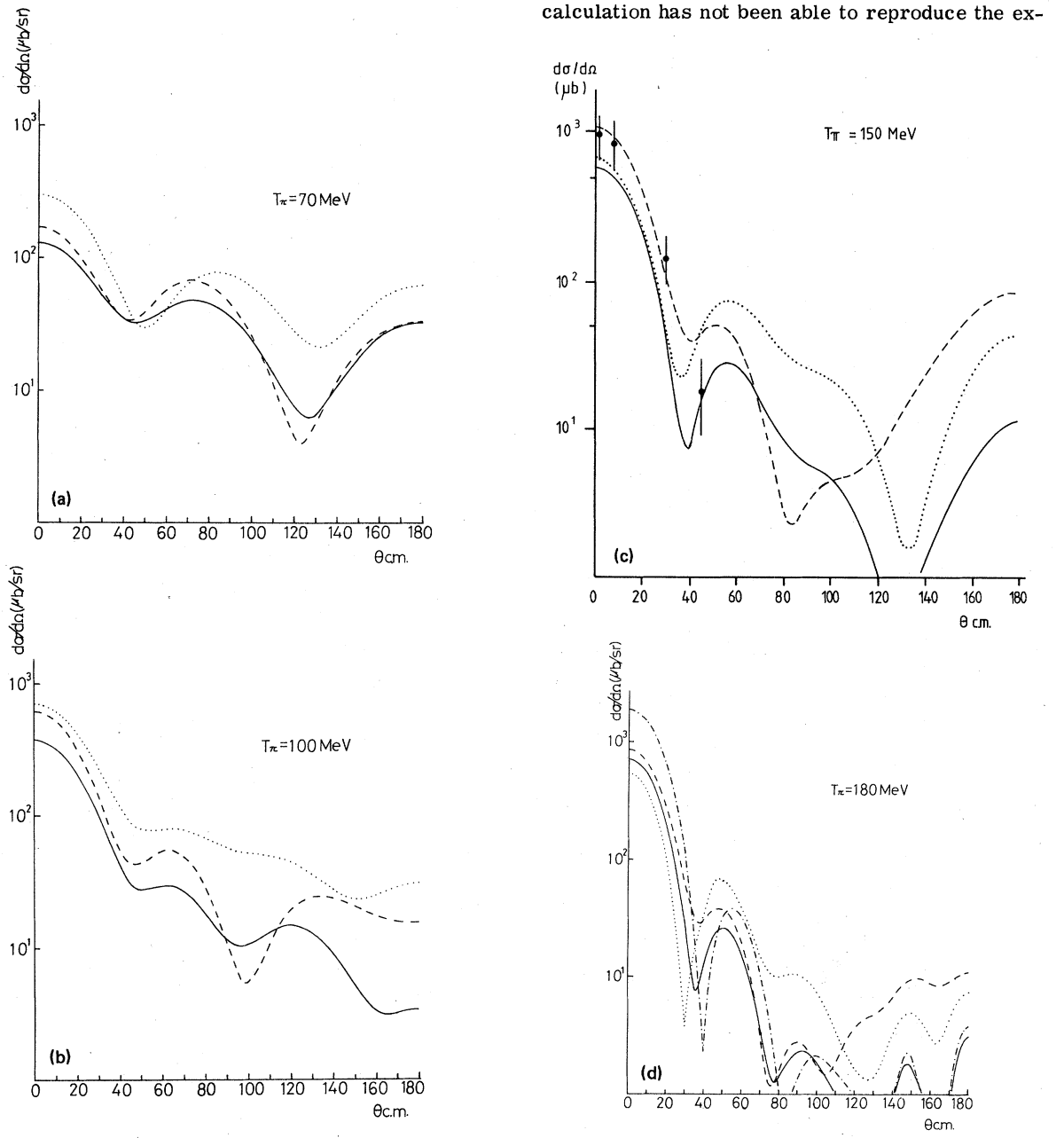

FIG. 5. The angular distributions of the $^{13}C(\pi^+, \pi^0)^{13}N_{g.s.}$ charge exchange scattering. The data in (c) are from Ref. 20. The dash-dotted line in (d) corresponds to $W_s^{3/2} = -30 - i47$ MeV and $W_s^{1/2} = -21 - i66$ MeV. Other lines are the same as in Fig. 4.

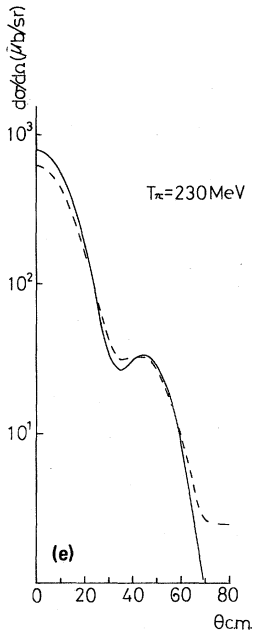

FIG. 5. *(Continued)*.

perimental values.

Let us now discuss the angular distribution. The calculated results are shown in Fig. 5. The definitions of the dotted, dashed, and solid lines are the same as those in Fig. 4. Unfortunately, up to now an angular distribution is observed only at the pion kinetic energy 150 MeV, and also has been measured only at four angles.[21] At 150 MeV the dashed line agrees reasonably with the experiment. This may be rather accidental. The important point is that both the shapes of the solid and dashed lines are not very different from each other up to 60°, although the absolute values of the cross sections are different. The introduction of the spreading potential into the propagator for the single Δ states leads to the damping of the CE transition amplitude, roughly speaking. In general, the contributions from the lower pion partial waves $(0^-, 1^+, 2^+)$ are larger in the nonstatic treatment than in the static treatment, because the pion can get more deeply into the inside of the nucleus due to the Δ-hole propagation. The angle of the first minimum in the angular distribution is about 10° larger in the nonstatic treatment than in the static treatment.

Let us consider the case where $W_s^{3/2}$ is not equal to $W_s^{1/2}$. The difference between $W_s^{3/2}$ and $W_s^{1/2}$ has to be made large to obtain a close cross section to the observed value. For example, at the pion kinetic energy 180 MeV, $u_s^{3/2}+iv_s^{3/2}$ and $u_s^{1/2}+iv_s^{1/2}$ become $-30-i47$ and $-21-i66$ MeV, respectively, to obtain the integrated cross section of 0.7 mb. The angular distribution of the elastic scattering obtained by this choice for $W_s^{3/2}$ and $W_s^{1/2}$ is little different from the one calculated by taking $W_s^{3/2} = W_s^{1/2}$. In the CE scattering the absolute values of the cross sections are very different from each other as a matter of course, and the angle of the first minimum in the former shifts to the larger angle by about 5° more than the one in the latter. This difference between $W_s^{3/2}$ and $W_s^{1/2}$ is very large. The difference between $W_s^{3/2}$ and $W_s^{1/2}$ may become large because here the whole effects which contribute to the increase of the cross section are artificially charged to the self-energy (the spreading potential) of the delta. In this paper the important charge exchange mechanisms, as shown in Fig. 6, were not taken into account. The pion can exchange the charge with the nucleon outside the closed shell through the true pion absorption and the multiple reflection. The diagrams in Fig. 6 cannot be described by the self-energy form of the delta. If the contributions of these diagrams are taken into account, the difference between $W_s^{3/2}$ and $W_s^{1/2}$ may be reduced.[22]

IV. SUMMARY

The transition matrix in the pion-nucleus system to the isobaric analog state between the mirror nuclei was described on the same level as the elastic scattering formulation by using the delta-hole formalism. If the binding correction, the Pauli-quenching correction, and the spreading potential are taken into account all together, the calculated excitation function of the $^{13}C(\pi^+, \pi^0)^{13}N_{g.s.}$ CE scattering cross section becomes flat, and the shape of the calculated angular distribution at the pion kinetic energy 150 MeV is reasonably consistent with the experimental data. However, the magnitude of the integrated cross section is roughly factor of 3 less than the experimental value (about 1 mb). We examined how large the integrated cross section becomes when the spreading potential $W_s^{3/2}$ of the isospin $\frac{3}{2}$ is not equal to the spreading potential $W_s^{1/2}$ of the isospin $\frac{1}{2}$. It was

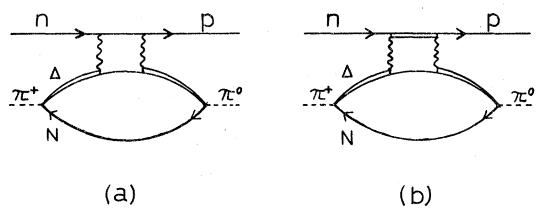

FIG. 6. The pion-nucleus charge exchange diagrams being brought about by the true pion absorption (a) and the multiple reflection (b).

necessary to make the difference between the spreading potentials $W_s^{3/2}$ and $W_s^{1/2}$ large to reproduce the observed cross section. The additional charge exchange mechanism which may be able to reduce the difference between the spreading potentials $W_s^{3/2}$ and $W_s^{1/2}$ was discussed.

Note added. Recently, the DWBA treatment based on the delta-hole formalism has been performed for the $^{15}N(\pi^+, \pi^0)^{15}O_{g.s.}$ charge exchange scattering, and the flat excitation function has been obtained between the pion kinetic energies 140 and 230 MeV, although the big bump appears around 100 MeV.[23]

ACKNOWLEDGMENTS

I am very grateful to Professor H. Narumi, and especially to Dr. F. Lenz, Dr. M. Thies, and Dr. T. Fujita for many fruitful discussions and comments. I am very grateful to the Schweizerisches Institut fur Nuklearforschung, and especially to Dr. F. Lenz and Dr. M. P. Locher for giving me the opportunity to stay at SIN.

[1]Y. Shamai *et al.*, Phys. Rev. Lett. 36, 82 (1976).
[2]N. Auerbach and J. Warszawski, Phys. Lett. 45B, 171 (1973); Nucl. Phys. A276, 402 (1977).
[3]D. Tow and J. M. Eisenberg, Nucl. Phys. A237, 441 (1975).
[4]W. R. Gibbs *et al.*, Phys. Rev. Lett. 36, 85 (1976).
[5]E. Oset, Phys. Lett. 65B, 46 (1976).
[6]H. Nishimura and K. Kubodera, Prog. Theor. Phys. 56, 986 (1976).
[7]G. A. Miller and J. E. Spencer, Ann. Phys. (N.Y.) 100, 562 (1976).
[8]K. P. Lohs and A. Gal, Nucl. Phys. A292, 375 (1977).
[9]J. Warszawski, A. Gal, and J. M. Eisenberg, Nucl. Phys. A294, 321 (1978).
[10]J. Alster and J. Warszawski, Phys. Rep. 52, 87 (1979).
[11]F. Lenz, Ann. Phys. (N.Y.) 95, 348 (1975).
[12]M. Hirata, F. Lenz, and K. Yazaki, Ann. Phys. (N.Y.) 108, 116 (1977); M. Hirata, J. H. Koch, F. Lenz, and E. J. Moniz, *ibid.* 120, 205 (1979).
[13]L. S. Kisslinger and W. L. Wang, Phys. Rev. Lett. 30, 1071 (1973); Ann. Phys. (N.Y.) 99, 374 (1976).
[14]N. Auerbach, Phys. Rev. Lett. 38, 804 (1977).
[15]E. Oset and W. Weise, Nucl. Phys. A319, 477 (1979).
[16]A. N. Saharia and R. M. Woloskyn, Phys. Lett. 84B, 401 (1979).
[17]R. H. Landau and A. W. Thomas, Phys. Lett. 88B, 226 (1979).
[18]F. Binon *et al.*, Nucl. Phys. B33, 42 (1971).
[19]Y. Horikawa, F. Lenz, and M. Thies, Nucl. Phys. A345, 386 (1980).
[20]This point was confirmed by M. Thies.
[21]J. D. Bowman, *Proceedings of the 8th International Conference on High-Energy Physics and Nuclear Structure, Vancouver, 1979,* edited by D. F. Measday and A. W. Thomas (North-Holland, Amsterdam, 1980), p. 375.
[22]The contributions of Fig. 6 are being estimated now by F. Lenz, M. Thies, and M. Hirata.
[23]E. Oset, Nucl. Phys. A356, 413 (1981).